(14) ERADCOM

(12) LEVEL II

ASL-TR-0042

AD

Reports Control Symbol
OSD 1366

(9) Research and development technical rept.

(6)

THE VISIOCEILOMETER: A PORTABLE CLOUD HEIGHT AND VISIBILITY INDICATOR

(11) OCTOBER 1979

(12) 40

By
(10) Robert S. Bonner
William J. Lentz

US Army Electronics Research and Development Command
ATMOSPHERIC SCIENCES LABORATORY
White Sands Missile Range, NM 88002

NOTICES

Disclaimers

The findings in this report are not to be construed as an official Department of the Army position, unless so designated by other authorized documents.

The citation of trade names and names of manufacturers in this report is not to be construed as official Government indorsement or approval of commercial products or services referenced herein.

Disposition

Destory this report when it is no longer needed. Do not return it to the originator.

REPORT DOCUMENTATION PAGE		READ INSTRUCTIONS BEFORE COMPLETING FORM
1. REPORT NUMBER ASL-TR-0042	2. GOVT ACCESSION NO.	3. RECIPIENT'S CATALOG NUMBER
4. TITLE (and Subtitle) THE VISIOCEILOMETER: A PORTABLE CLOUD HEIGHT AND VISIBILITY INDICATOR		5. TYPE OF REPORT & PERIOD COVERED R&D Technical Report
		6. PERFORMING ORG. REPORT NUMBER
7. AUTHOR(s) Robert S. Bonner William J. Lentz		8. CONTRACT OR GRANT NUMBER(s)
9. PERFORMING ORGANIZATION NAME AND ADDRESS Atmospheric Sciences Laboratory White Sands Missile Range, NM 88002		10. PROGRAM ELEMENT, PROJECT, TASK AREA & WORK UNIT NUMBERS DA Task 612111H710011.A3
11. CONTROLLING OFFICE NAME AND ADDRESS US Army Electronics Research and Development Command Adelphi, MD 20783		12. REPORT DATE October 1979
		13. NUMBER OF PAGES 27
14. MONITORING AGENCY NAME & ADDRESS(if different from Controlling Office)		15. SECURITY CLASS. (of this report) UNCLASSIFIED
		15a. DECLASSIFICATION/DOWNGRADING SCHEDULE

16. DISTRIBUTION STATEMENT (of this Report)

Approved for public release; distribution unlimited.

17. DISTRIBUTION STATEMENT (of the abstract entered in Block 20, if different from Report)

18. SUPPLEMENTARY NOTES

19. KEY WORDS (Continue on reverse side if necessary and identify by block number)

Ceiling
Visibility
Portable
Lidar

20. ABSTRACT (Continue on reverse side if necessary and identify by block number)

The first experimental prototype (model-1) visioceilometer has been developed. It measures cloud height from 50 to 3000 meters with 10-meter accuracy and calculates visibility from a sample volume up to 1 kilometer in length of the lidar return. It consists of a hand-held, battery-operated lidar which uses the AN/GVS-5 laser rangefinder optics. Measurements of visibility in fog and cloud ceiling height in clear air and rain were taken at the fog dispersion test facility at Otis Air Force Base (AFB) MA. In relatively homogeneous fogs,

20. ABSTRACT (cont)

the visibility accuracy was comparable to standard transmissometers. The cloud ceiling accuracy was also comparable to the standard rotating beam ceilometer, (RBC).

CONTENTS

FIGURES

INTRODUCTION

The importance of visibility to the Field Army has long been recognized. Electro-optic based weapon systems such as Copperhead have ceiling and visibility requirements, but accurate measurements are often difficult. Standard airport visibility measuring transmissometers are bulky, heavy, and are bistatic devices. The difficulty of making measurements in this manner for slant visual range is apparent. It is not always possible to place devices at both ends of a meaningful path even for horizontal measurements. Lidars, or laser radars, offer a potential solution to the problem of measuring visibility since they are monostatic devices which can probe the atmosphere from one location. Recent advances in technology enable the size of lidars to be reduced from large research devices to instruments not much larger than a pair of binoculars.

In November 1975, tests were conducted at Randolph AFB, San Antonio, Texas, to evaluate the performance of the AN/GVS-5 laser rangefinder as a portable, hand-held battery-operated cloud height indicator.[1] The laser rangefinder measurements compared to those of the RBC for 63 hourly samples from 28 November to 15 December 1975 produced a calculated linear least squares correlation coefficient of 0.77. A recommendation was then made to produce a combined hand portable ceiling and visibility sensor in one package. With this in mind, a joint development effort[2] was initiated with the Laser Division of the Night Vision and Electro-Optics Laboratory at Fort Monmouth, New Jersey, to add visibility measuring capability to the rangefinder. The result of this joint development and the subject of this report are the model-1 visioceilometer and its evaluation at the Otis AFB Fog Dispersion Test Facility.

VISIBILITY DEFINITION

Visibility as observed by the human eye is a very complex parameter depending on many factors other than the obscuring medium. Before any use can be made of a given measurement of visibility, it is important to select a definition which can be related to a variety of instruments as well as the human eye. For example, a standard airport transmissometer is said to measure visibility, but in actuality it measures transmission between two points. Under the same conditions it will indicate the same visibility at day or night even though the human eye might define the visibility as quite different. Nevertheless, the transmissometer measurement of visibility can

---

[1]R. S. Bonner and R. Newton, 1977, "Application of the AN/GVS-5 Laser Rangefinder to Cloud Base Height Measurements," ECOM-5812, Atmospheric Sciences Laboratory, White Sands Missile Range, NM

[2]Henry Saphow, Fred Kolylarz, Gunther Kaindz, and Earl Griggs, 1979, "The Visioceilometer (XE1) ANGMQ ( ) (Visibility and Ceiling Sensor)," draft report, US Army Electronics Command, Fort Monmouth, NJ

be related to how far the eye can discern a standard target in daylight or how distant a given light may be seen at night. Middleton[3] has defined the meteorological range or visual range V_r to be

$$V_r = \frac{-\ln(0.02)}{\sigma} , \tag{1}$$

where 0.02 is a minimum contrast threshold for standard target detection by eye and σ is the extinction coefficient per meter.

The contrast threshold has been accepted by the World Meteorological Organization and the US Air Force Air Weather Service for measurements in fog as 0.05 which yields a visual range of

$$V_r = \frac{-\ln(0.05)}{\sigma} . \tag{2}$$

For the purpose of this report, the visibility will be defined to be the visual range as defined in equation (2) whether observed by the human eye or measured by an instrument.

VISIBILITY CALCULATION

As the light from a lidar passes through an obscuring medium, the light is both scattered and absorbed. The formula governing the energy received by the lidar receiver is given by the lidar equation

$$P_r(r) = P_t\, K\, \frac{c\tau}{2} \frac{A_r}{r^2}\, \beta(r)\, t_c(r)\, \exp\left[-2\int_0^r \sigma(r)dr\right] , \tag{3}$$

where

$P_r(r)$ = power collected (from a given range r)

K = lidar-system efficiency

r = range

P_t = power transmitted

c = velocity of light

τ = pulse duration

A = receiver area

---

[3] W. E. K. Middleton, 1963, Vision Through the Atmosphere, Toronto Press, Toronto, Canada

$\beta(r)$ = backscatter coefficient (m^{-1})

$t_c(r)$ = beam convergence factor

$\sigma(r)$ = volume extinction coefficient

For the purpose of analysis, all of the constants and known functions can be combined to reduce the form of the equation to

$$P_r(r) = \frac{\xi\beta(r)}{r^2} e^{-2\bar{\sigma}_r r}, \text{ where } \bar{\sigma}_r = \frac{\int_0^r \sigma(r)\,dr}{r} \qquad (4)$$

and ξ is the combination of constants and known functions. In this simplified formula, the energy returned to the receiver from a range r is proportional to the backscatter coefficient $\beta(r)$ at r and inversely proportional to r^2.

At this point one has an exact equation with two unknowns which cannot be solved without further knowledge or assumption. If the transmissivity is measured, then $\bar{\sigma}_r$ would be known, but this requires a double ended device and negates the purpose of using a lidar. Assuming that only the single lidar return is known, then the simpliest course is to assume a homogeneous atmosphere.

Following Viezee,[4] the term S(r) is defined:

$$S(r) = 10 \log_{10} \frac{P_r(r)\ r^2}{P_r(r_0)\ r_0^2}, \qquad (5)$$

where r_0 is a reference range and is constant. The derivative of S(r) over the range of full beam crossover is then:

$$\frac{dS}{dr} = 4.34 \frac{1}{\beta(r)} \frac{d\beta(r)}{dr} - 8.7\ \sigma(r)\ . \qquad (6)$$

[4]William Viezee et al, 1972, Slant Range Visibility Measurement for Aircraft Landing Operations," AFCRL-72-DI54, Air Force Cambridge Research Laboratories, Bedford, MA

When the backscatter coefficient $\beta(r)$ is independent of range as in the homogeneous scattering medium

$$\overline{\sigma}_r = \frac{-1\Delta \quad S}{8.7\Delta \; r} = m = \text{slope} \; . \tag{7}$$

Then $\overline{\sigma}_r$ is the slope of the plot of S(r) versus r and is obtainable directly from the lidar returns. Viezee et al[5] have used this relation when $\frac{\Delta S}{\Delta r} < 0$. A more complete discussion of the errors and limitations on the technique is found in Viezee.[6]

To determine an accurate value of $\overline{\sigma}_r$, a least squares linear fit is made to the S(r) line to minimize the errors due to random noise and small inhomogeneities. The closeness of the fit also indicates how valid the homogeneity assumption is. This technique is readily adapted to computer analysis and was used to process the Otis AFB lidar returns for comparison to other visibility instrumentation.

MULTIPLE SCATTERING

In the preceding analysis, the assumption was made that the lidar return was composed solely of singly scattered photons. In very dense fogs this may not be the case. The parameters used in a study[7] performed to determine the effects of multiple scatter in fogs on the model-1 visioceilometer are shown below:

Wavelength	1.06μm	Beam 1/2 angle 0.5 mr
Energy	10 mj	Receiver size 2.857 cm
Pulse length	6 ns	Receiver 1/2 angle 1.5 mr
Source size	0.8 cm	Source-receiver separation 12.065 cm

---

[5]W. Viezee, E. Uthe, and R. T. H. Collis, 1969, "Lidar Observations for Airfield Approach Conditions: An Exploratory Study," JAM, 2:274-283

[6]W. Viezee, L. Oblanas, and R. T. H. Collis, 1973, "Evaluation of the Lidar Technique of Determining Slant Range Visibility for Aircraft Landing Operations," AFCRL-TR-73-0708, Air Force Cambridge Research Laboratories, Bedford, MA

[7]W. G. M. Blattner and C. M. Lampley, 1977, "Multiple Scattering Effects for Backscatter Lidar System at WSMR," Radiation Research Associates, RRA-47706, Fort Worth, TX

Figure 1 shows the effects of multiple scatter in fog on the visioceilometer receiver for a visibility of 100 meters. The three histograms are statistically derived results of multiple scattering calculations for single scattering, double scattering, and triple scattering. The smooth curve is calculated from the lidar equation by using the theoretical extinction and backscatter coefficients used in the multiple scatter calculations. Both the total and single scattering histograms agree well with the lidar equation with the exception of the early returns which are much larger than predicted by the lidar equation. Since multiple scattering is most important for low visibilities, figure 1 indicates the relative importance of multiple scattering.

The important result to visibility calculations is the conclusion that multiple scattering will only affect the slope technique slightly for low visibilities. In the 100- to 300-meter range for some fog models, the error in a least squares fit will be in the range of 5 to 10 percent. An important practical consideration is that both the peak height and the time of the peak of the lidar return are very different from the singly scattered return. The early returns are much larger than those predicted by the lidar equation, and these signals may overload the detector of the lidar and cause the later returns to be useless.

POTENTIAL USES

The model-1 visioceilometer (figures 2 and 3) is quite different from research lidars in that it contains a complete transient recorder and processing electronics in less than 1 cubic foot. It is designed to be completely automatic after the laser is fired and can be used with a minimum of training. It can be used in lieu of observer estimates of prevailing visibility at any weather observation station such as those of the Air Weather Service, Federal Aviation Agency, National Weather Service, and Navy. It can be used at remote airfields where cloud height and visibility measurements are required but where standard instruments are too inconvenient. An applied tactical use for this type of instrument would be at Army Division Artillery meteorological sections in lieu of visual observations and ceiling balloons. At present, the Navy has no accurate means of determining visibility or cloud height from its ships at sea. This device could provide a convenient means of making these measurements.

DEVICE DESCRIPTION

The model-1 visioceilometer uses the hand-held, battery-operated AN/GVS-5 laser rangefinder as a laser source for the ceiling and visibility detector. The laser emits a single 1.06-micrometer pulse averaging 10 millijoules in 6 nanoseconds. The backscattered atmospheric return produced by the interaction of the atmosphere and the laser pulse is detected in a 1.06-micrometer filtered photoavalanche detector which is temperature compensated for constant gain. Lidar returns from up to 3 kilometers are compressed by a

video logarithmic amplifier from four decades of input to two decades of output with 35 megahertz bandwidth. The compressed return is digitized to 12 bits by a 20-megahertz sampling rate transient recorder which has 455 sample points. The digitized return is fed serially into a mini-computer which calculates visibility or cloud ceiling height (figure 4).

TRANSIENT RECORDER

The heart of the visioceilometer is its transient recorder. The ability to capture a single lidar pulse return and digitize it for conversion to visibility is unique in a hand portable device. To do this, a charge coupled device (CCD) was chosen to slow the lidar return down to a rate at which a low power analog to digital converter (ADC) could digitize the return. The CCD allows the lidar return to be sampled at up to 20 megahertz and fed out at 44 kilohertz to the ADC. The 20-megahertz sample rate corresponds to a sample every 7.5 meters on the lidar return, and 44 kilohertz corresponds to a reliable digitization rate in a 12 bit ADC.

Functionally, the CCD is a sequence of sample and hold circuits which pass the sample input from the input to the next sample and hold as packets of charge. For this reason, the CCD is sometimes referred to as a "bucket brigade." The main advantage of the CCD is its extremely fast acquisition time. In many cases it is limited only by the clock shift transition time which may be as small as a few nanoseconds. The main disadvantage of CCD is that the signals decay through leakage of charge in the registers. At temperatures above 23° Celsius the signal may decay away before it shifts out of the CCD. This thermal decay is displayed as a gradual decreasing baseline on the return signal plot (figures 5 and 9).

The CCD thermal decay can be separated from the lidar return, however, by a curve fit to the points beyond where the signal-to-noise ratio becomes one. The fit is a polynomial of the form $P_r(r) = a + br + cr^2$ where a, b, and c are constants. A fit is made to every lidar return from sample 80 to sample 100, and the result is extrapolated over the entire curve to remove thermal decay.

In like manner, the system nonlinearities are removed by a polynomial fit to a calibration curve. The calibration curve was obtained by measuring the digital values produced by test voltages (figure 5). Figure 6 shows the resulting calibration curve generated by making a ninth degree least squares polynomial fit to the log of the digital output versus the voltage input. Each sample point of the lidar return must be calculated through the ninth degree polynomial to obtain the actual lidar return independent of circuit nonlinearities. Both the calibration curve and decay curve fitting introduce unnecessary programming complications which will be eliminated in the second experimental prototype visioceilometer (model-2).

ANCILLARY DATA SYSTEMS

To properly evaluate the model-1 visioceilometer and gain a data base on which to build improved visibility algorithms, a ceiling and visibility evaluation system (CAVES) was constructed in a 32-foot van. The CAVES consists of a Nova 3 minicomputer for data gathering and interfaces to various visibility and meteorological instruments. The main purpose of the Nova 3, however, is to automatically fire the visioceilometer, store its lidar returns, and convert the returns to visibility. Real-time plots of the lidar data also ensure the validity of the data.

EXPERIMENT DESCRIPTION

In May 1978 an experiment was conducted at Otis AFB, MA, to compare the performance of the model-1 visioceilometer to that of a 152-meter path transmissometer[8] and to that of the EG&G forward scatter meter (FSM)[9,10] for visibility determinations. In addition, cloud height measurement comparisons were made between the visioceilometer, the AN/GVS-5 laser rangefinder, and the AN/GMQ-13A RBC. Figure 7 shows a top view of the relative positions of the instruments. The path between the transmissometer projector and receiver was parallel to the beam path of the visioceilometer, separated horizontally by approximately 6 meters and vertically by approximately 2 meters. The EG&G FSM was located about midway on the length of the path of the transmissometer, separated horizontally from the transmissometer path by 1 meter, and at the same height above the ground as the transmissometer. For cloud height measurements, the visioceilometer was removed from the top of the Atmospheric Sciences Laboratory (ASL) van and placed 1 meter horizontally from the RBC receiver and at the same level above the ground (figure 8).

The Naval Research Laboratory (NRL) provided several Knollenberg particulate counters and transmissometers with their own instrumented van[10] which was located approximately 7.5 meters from the ASL van. The size distributions from these particle counters can be used with Mie theory to calculate a theoretical extinction and backscatter coefficient against which the transmissometers and lidars can be compared. Even more important is the data base for comparisons from which improved future designs of lidars can benefit.

---

[8]C. A. Douglas and R. L. Booker, 1977, "Visual Range: Concepts, Instrumental Determination, and Aviation Applications," FAA-RD-77-8, AD A 041098

[9]Wayne S. Hering and E. B. Geilser, 1978, "Forward Scatter Meter Measurements of Slant Visual Range," AFGL-TR-78-0191, Air Force Geophysical Laboratory, Hanscom AFB, MA

[10]Wayne S. Hering, H. S. Muench, and H. A. Brown, 1971, "Field Test of a Forward Scatter Visibility Meter," AFCRL-71-0315, AD726995, Air Force Cambridge Research Laboratories, Bedford, MA

DATA COLLECTION

On 17 May 1978 data were collected during the period 0651 to 0726 local time from the visibility instruments described in the experiment description. This fog was at least 60 meters thick at 0651 because forward scatter meters mounted at 61 meters on towers near the experiment were indicating 0.15 kilometer visibility. The visibility decreased at the 61-meter level until the end of the sampling period where it was 0.09 kilometer. Winds were 1 to 2 miles per hour for the entire sampling period over the entire vertical interval from 3 to 61 meters.

Wind data were recorded on 17 May 1978 from an instrument located within 10 meters of a line between the transmissometer projector and detector and halfway between them. The anemometer was approximately 3 meters above the surface. The data are shown in table 1.

TABLE 1. WINDS DURING FOG VISIBILITY COMPARISON MEASUREMENTS
17 May 1978

Time	Speed (mph)	Dir	Time	Speed (mph)	Dir
0651	2	227	0709	2	205
0652	2	232	0710	1	214
0653	2	224	0711	2	210
0654	2	210	0712	2	215
0655	2	215	0713	2	198
0656	2	218	0714	1	187
0657	2	220	0715	1	196
0658	2	194	0716	2	203
0659	2	196	0717	2	215
0700	2	202	0718	1	208
0701	2	185	0719	1	197
0702	2	190	0720	2	208
0703	2	191	0721	2	241
0704	2	201	0722	1	233
0705	2	193	0723	2	221
0706	2	199	0724	1	223
0707	2	208	0725	1	234
0708	2	202	0726	1	201

On 24 May 1978 cloud height data were taken with the visioceilometer, the AN/GVS-5 laser rangefinder, and the RBC during the time interval 1724 to 1757. The data from the RBC were transmitted to an oscilloscope whose trace was recorded on video tape. In this manner a permanent record was made of each sampling of the cloud base by the RBC. The video tapes were later scanned for the RBC data and were reduced manually. Data from the AN/GVS-5 were recorded manually by observing the display in the eyepiece of the instrument and recording it on paper. The visioceilometer data were automatically stored in the computer system for later reduction.

RESULTS

Cloud Ceiling Measurements

By using the experimental setup described in figure 8, a comparison was made on 24 May 1978 at Otis AFB between several standard cloud height indicators and the model-1 visioceilometer. The RBC[11] is used at many airports and is the standard against which these comparisons were made. The ASEA type QL-1210 ceilometer[12] is a multiple pulse lidar for use up to 1000 meters with chart recorder output. The AN/GVS-5 rangefinder is a single pulse lidar for use in ranging solid targets from 100 meters to 10 kilometers. Its application to cloud measurements has been discussed in an earlier report.[1]

Several visioceilometer lidar returns from hard targets are shown in figure 9. In every case the range to targets agreed to within 10 meters with the AN/GVS-5 laser rangefinder which was previously calibrated against measured distance targets and was as accurate as the measured distances. The dropout occurring from points 62 to 64 is caused by an internal fault in the CCD chip which is eliminated in processed data by the minicomputer. The slope of the lidar return is a combination of CCD decay and visibility attenuation. In visibility data, the CCD decay is eliminated by a second degree curve fitting to the tail of the return. In cloud height or target data, there is no need for this processing, so raw data curves are presented.

---

[11]G. L. Trusty and T. H. Cosden, 1979, "Optical Extinction Predictions from Measurements on the Open Sea," NRL Report 8260, Naval Research Laboratory, Washington, DC

[12]R. S. Bonner, SFC R. W. Carroll, and SP5 D. R. McWilliams, 1976, "Ceilometer, Type QL-1210, Ceiloskop, and Videograph B," Foreign Materiel Exploitation Report AST-1740A-096-76, White Sands Missile Range, NM

[1]R. S. Bonner and R. Newton, 1977, "Application of the AN/GVS-5 Laser Rangefinder to Cloud Base Height Measurements," ECOM-5812, Atmospheric Sciences Laboratory, White Sands Missile Range, NM

Figures 10 and 11 are typical stratus cloud returns as measured by the visioceilometer in light to moderate rain. In figure 10, there is little or no rain striking the ground in the area around the lidars, but in figure 11 there is light to moderate rainfall near the ground. This is shown by the series of sharp spikes in the return below 155 meters.

The visioceilometer could distinguish easily between rain and clouds by its reaction to the rain (small width pulses) and its reaction to the cloud base (wide pulse). However, the AN/GVS-5 laser rangefinder erroneously indicated the distance to the rain since it contains simple discriminator circuits which look for a threshold. Three types of errors were observed with the rangefinders:

1. Low range indications due to rain.

2. No range indication due to weak return or below minimum range capability signal.

3. High range indication due to signal attenuation and cloud penetration.

These errors may cause the indicated cloud height to be in error by a factor of two to three. A comparison of the cloud heights as measured by the RBC and the AN/GVS-5 laser rangefinder is shown in figure 12. Zero values indicate no return or below minimum range after repeated laser firings.

The RBC can also distinguish between rain and clouds, but a human interpretation is required which may vary greatly between observers. Nevertheless, the visioceilometer followed the RBC trace to within 120 meters maximum and 0 meters minimum separation as can be seen in figure 13 which is the same block of data as figure 12. No data were taken during the period between 1704 and 1720 minutes on the RBC. Most of the disagreement originated in uncertainties in human interpretation of the RBC display, and the visioceilometer is believed to be accurate to $\pm$10 meters for cloud ceilings.

Visibility Measurements

An example of the slope analysis of a single lidar return is shown in the processed lidar return of figure 14. The initial rise of the lidar signal is caused by the gradual overlap of the transmitter and receiver fields of view. The lidar return is set equal to zero at point 40 where the signal-to-noise ratio becomes one due to a detector threshold noise problem. A linear least squares fit is shown superimposed on the return, which is essentially what is shown in equation (5). The slope of the fitted line is inversely proportional to the visibility. Note that the steeper the fitted line, the lower the visibility. A nearly horizontal fitted line corresponds to clear air visibility. If the slope of the line is positive, the fog is increasing in

density quickly and the slope technique will not work. The extremely close fit of the return to a straight line indicates that this fog sample is very homogeneous and the assumptions are valid for the slope fit.

Figure 15 shows a plot of the visibility obtained during an episode of fog at the Otis AFB fog dispersion facility. The three lines correspond to visibility as calculated from the visioceilometer, a 152-meter path length transmissometer (AN/GMQ-10), and the EG&G forward scatter meter. The dashed line indicates periods when no data were taken on one or more of the comparison instruments.

The forward scatter meter has a time constant of 50 seconds on the output, and the transmissometer has a time constant of 10 seconds. This reduces the actual variability of the fog by averaging out the fluctuations. The visioceilometer, however, makes its measurement in about 5 microseconds and records a virtually instantaneous value of the visibility. For this reason, the visioceilometer shows more variability with time than the range instruments. This characteristic of the visioceilometer is more realistic in displaying the spatial and temporal variability of the fogs than the long time averaged devices.

FUTURE PLANS

The model-1 visioceilometer is presently being updated with a new CCD circuit. The new CCD circuit will not contain the dropout at points 62 to 64 and will be operated in a differential mode to eliminate the thermal decay problem. The transient recorder power will also be strobed to prolong battery life in the updated model-1.

An engineering design analysis has recently been concluded to determine the best design for an improved model-2 visioceilometer. The current model-1 prototype weighs 16 pounds and measures 12 inches long by 11-1/2 inches wide by 7 inches high. The new model-2 visioceilometer should be both smaller and lighter and have less power consumption. In addition, the model-2 will be in two packages connected by a cable (figure 16). The optical unit will be housed in an AN/GVS-5 case and weigh about 5 pounds. The transient recorder and microprocessor will be housed in a separate case about the same size as the AN/GVS-5 and weigh less than 6 pounds. These study estimates of the weight are expected to be reduced quite significantly in the final visioceilometer.

Improved algorithms for visibility inversions based on the Otis AFB test data have been developed and will be installed in the model-2 visioceilometer. They are currently operational in the CAVES minicomputer and will be used with the improved model-1 visioceilometer to gather further data for future refinements.

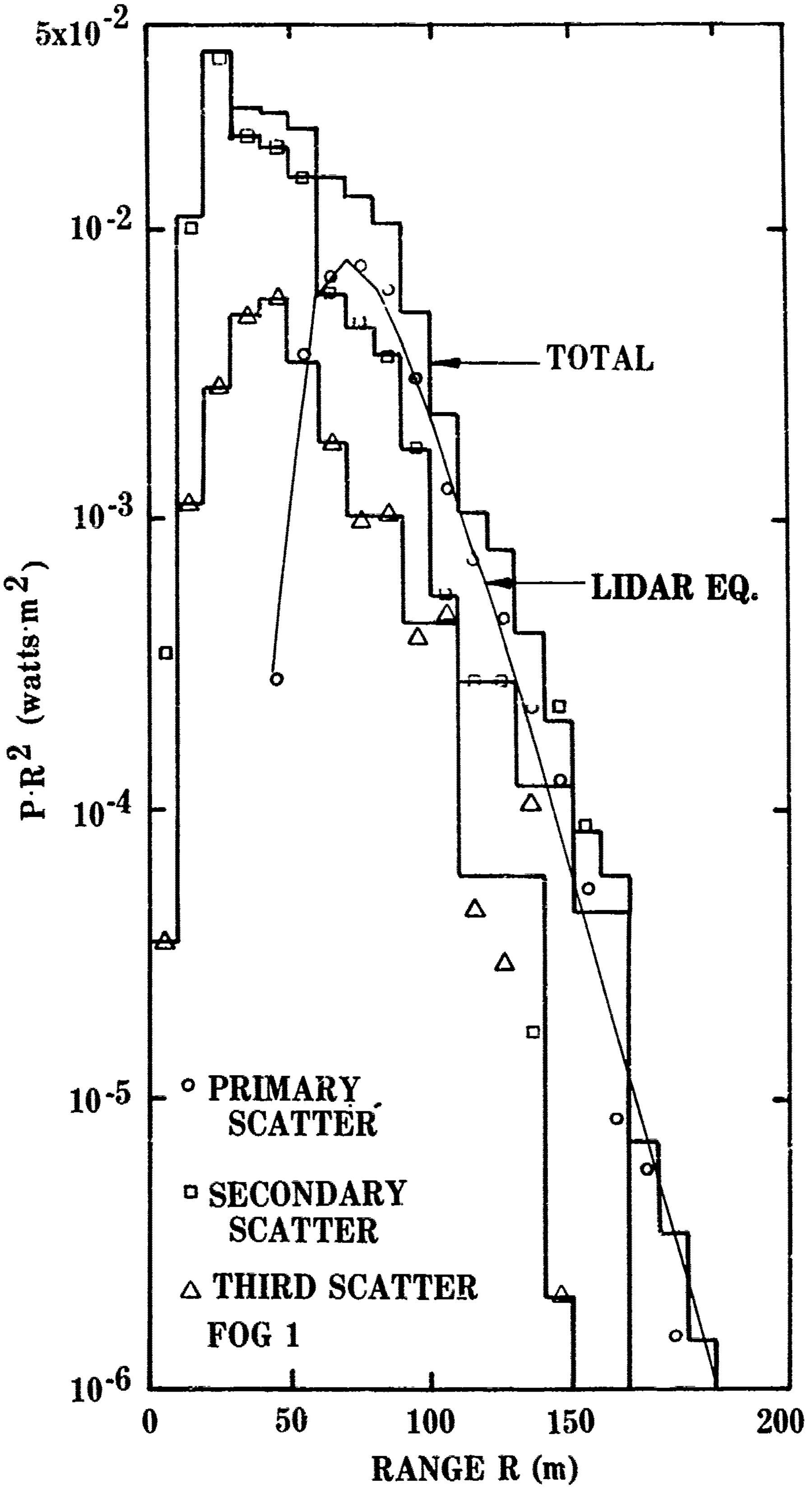

Figure 1. Receiver response for a visibility of 100 m.

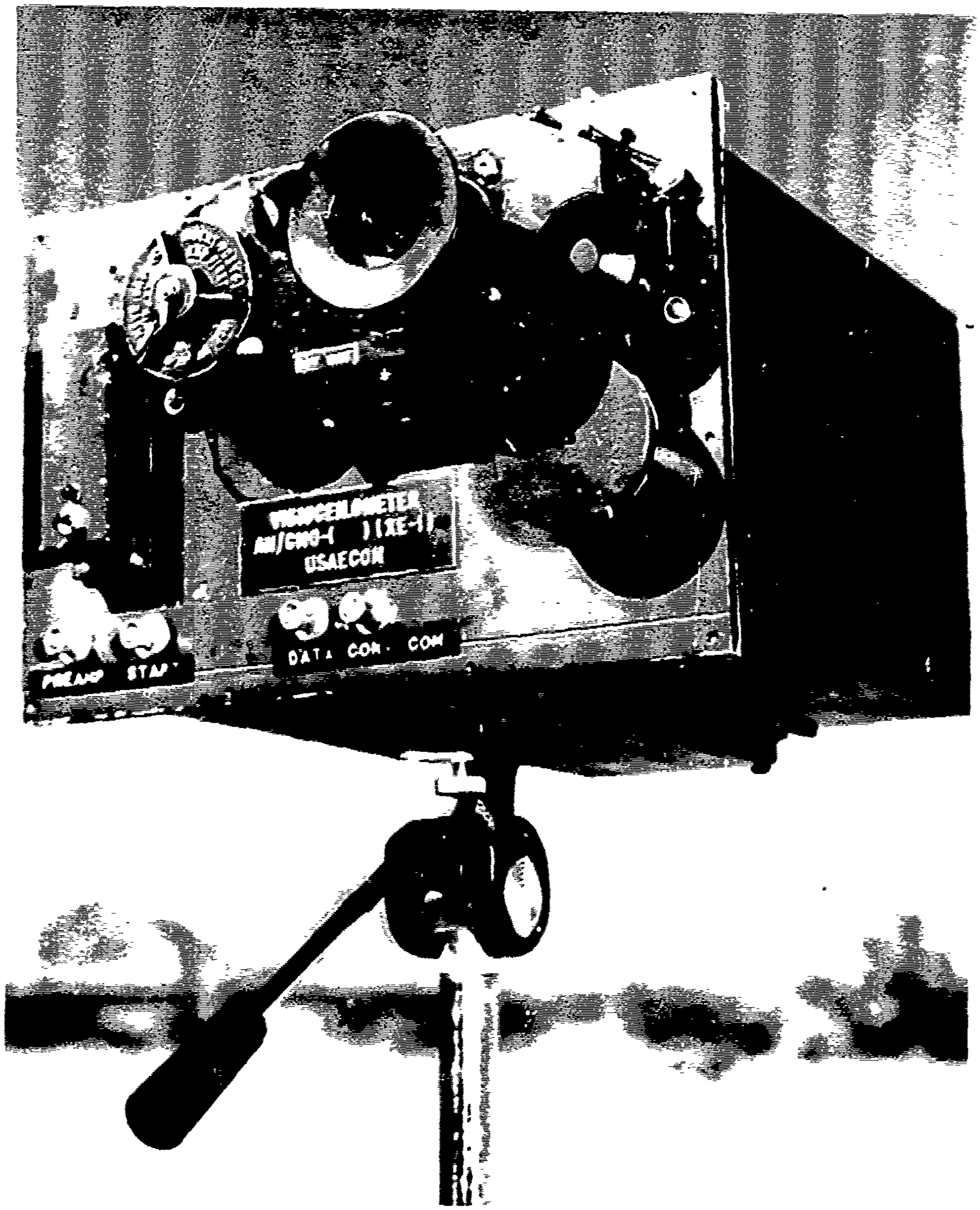

Figure 2. Operator view of model-1 visioceilometer.

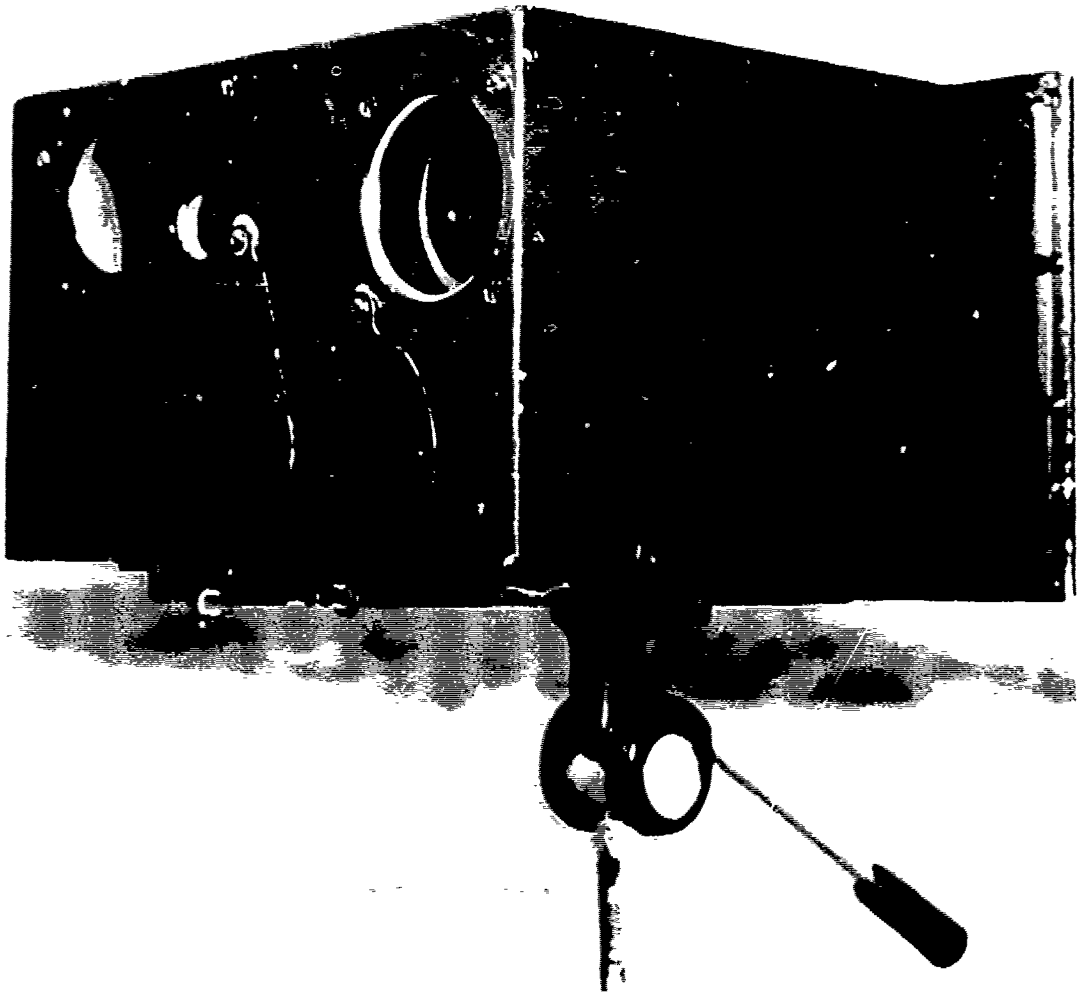

Figure 3. Optics side of model-1 visioceilometer.

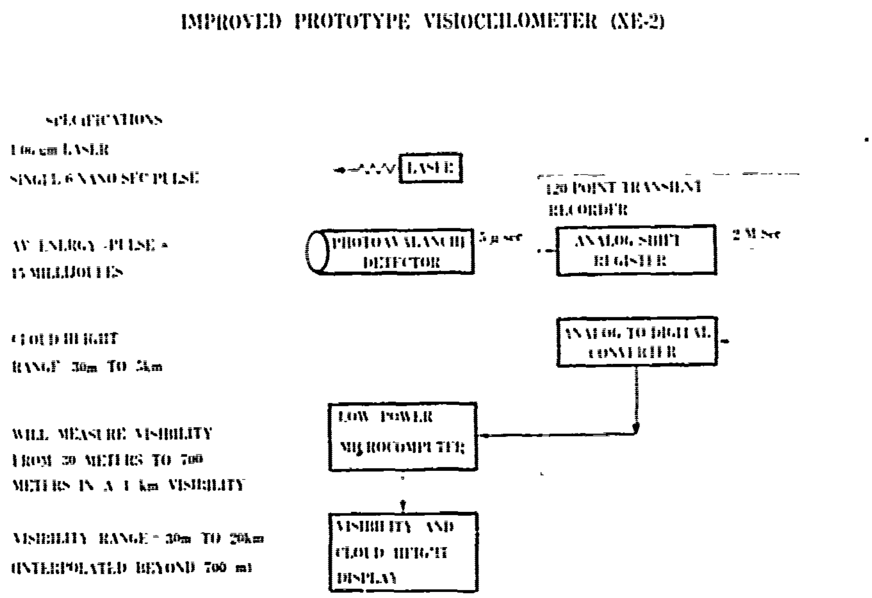

Figure 4. Block diagram of model-1 visioceilometer connected to minicomputer system.

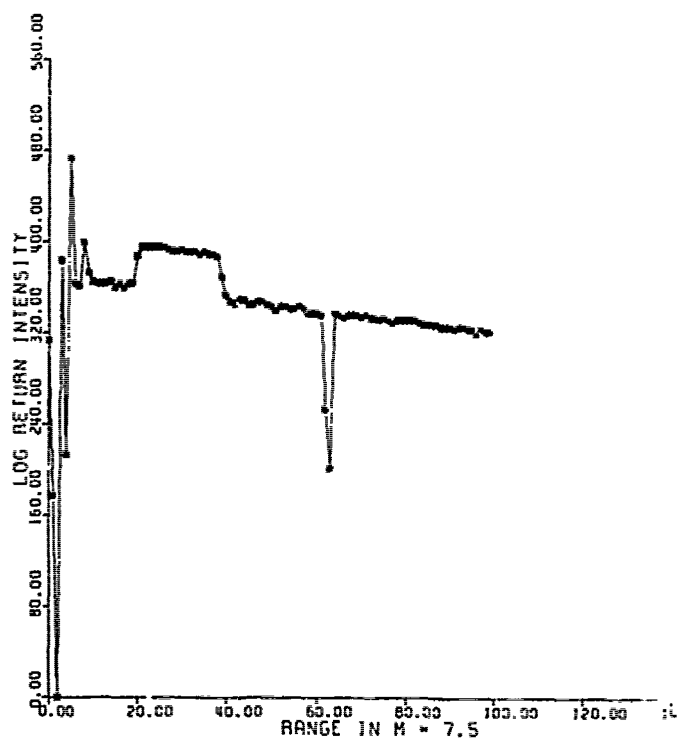

Figure 5. Response to input pulse with thermal decay (sloped baseline).

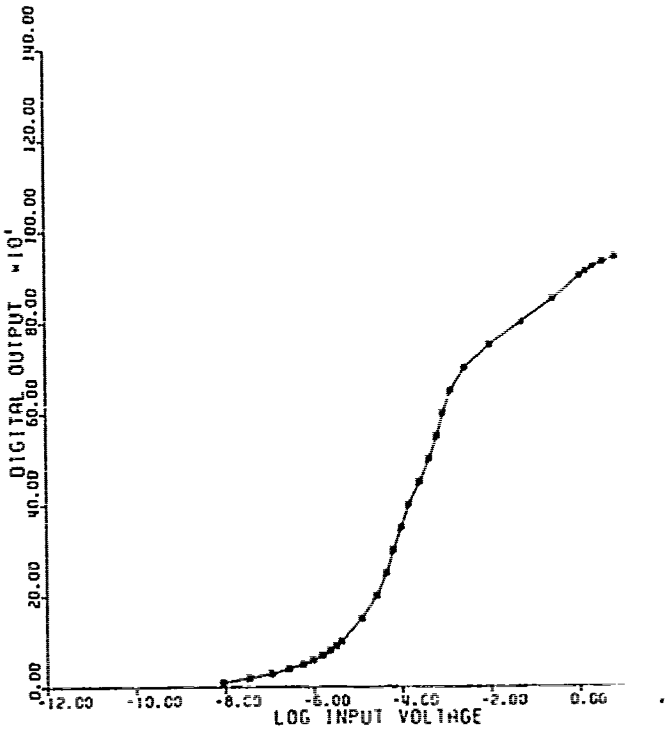

Figure 6. Calibration curve for model-1 visioceilometer.

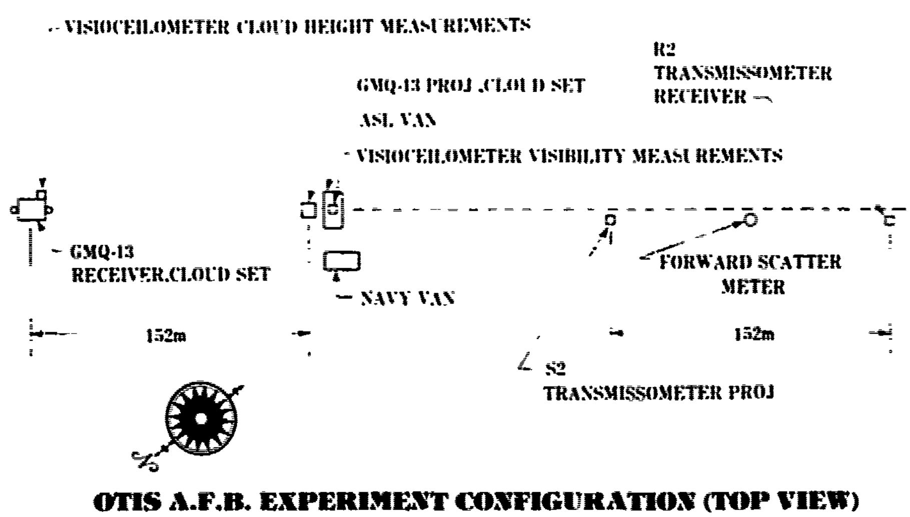

Figure 7. Otis AFB experiment configuration.

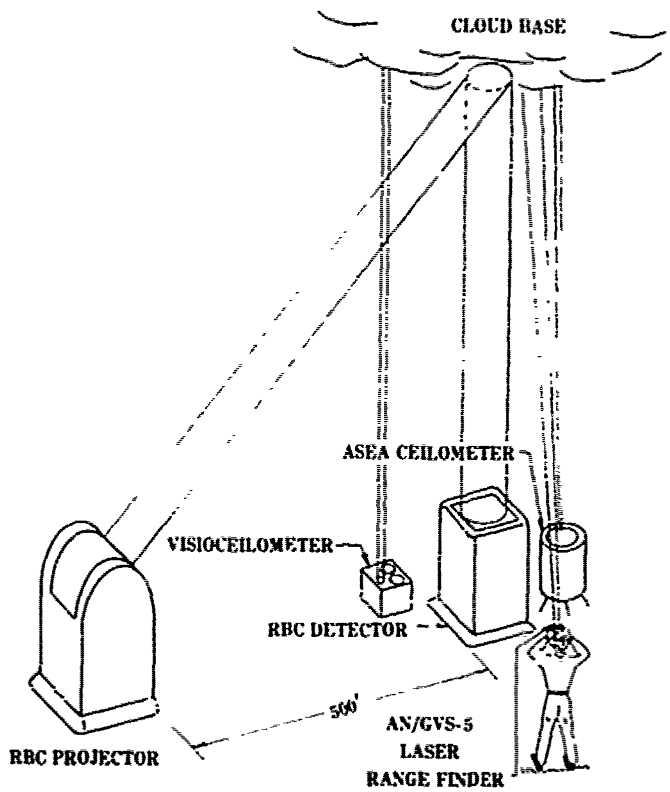

Figure 8. Experiment configuration for taking cloud height data at Otis AFB.

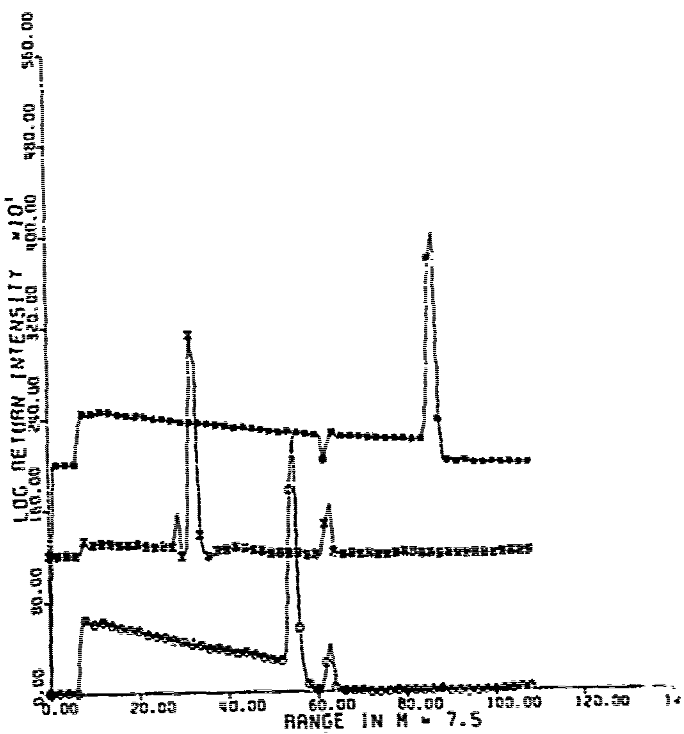

Figure 9. Visioceilometer returns from hard targets.

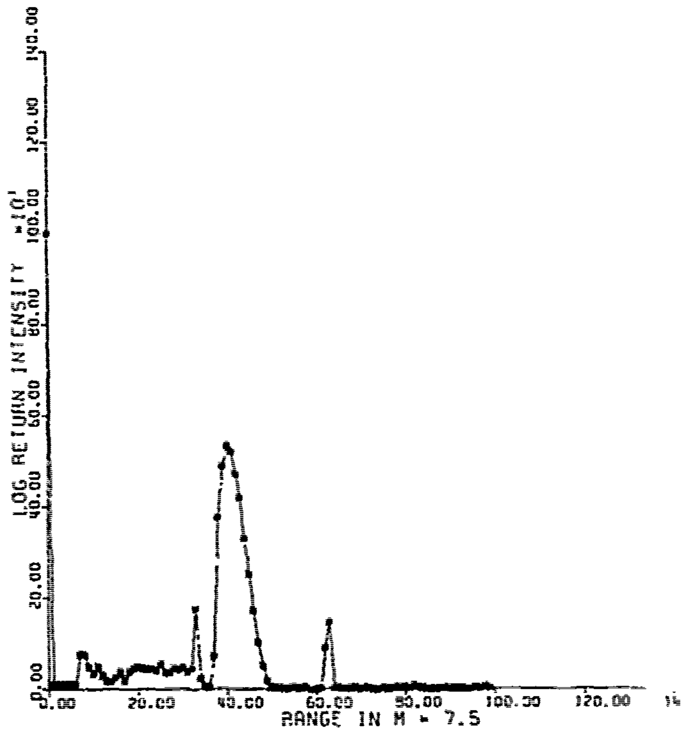

Figure 10. Visioceilometer cloud height return with indication of rain immediately below the cloud.

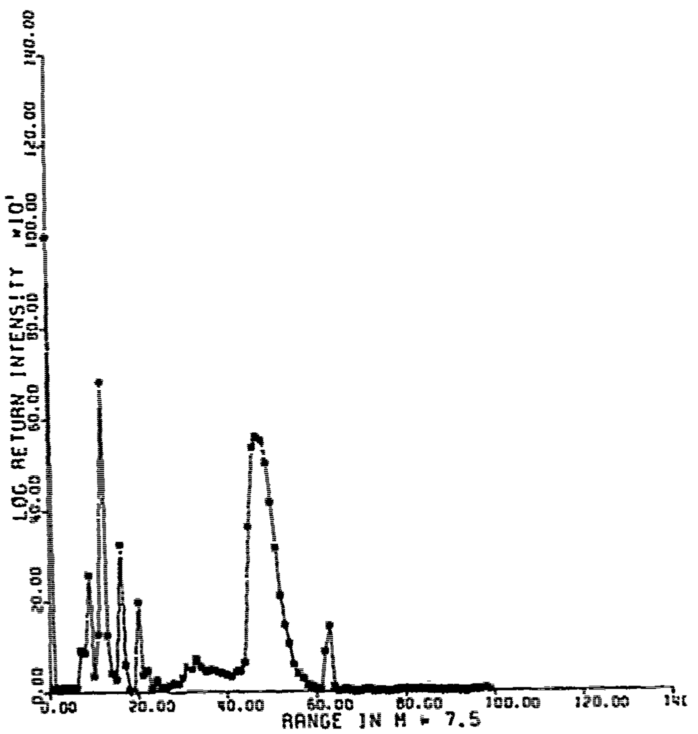

Figure 11. Visioceilometer cloud height return with rain immediately above the sensor.

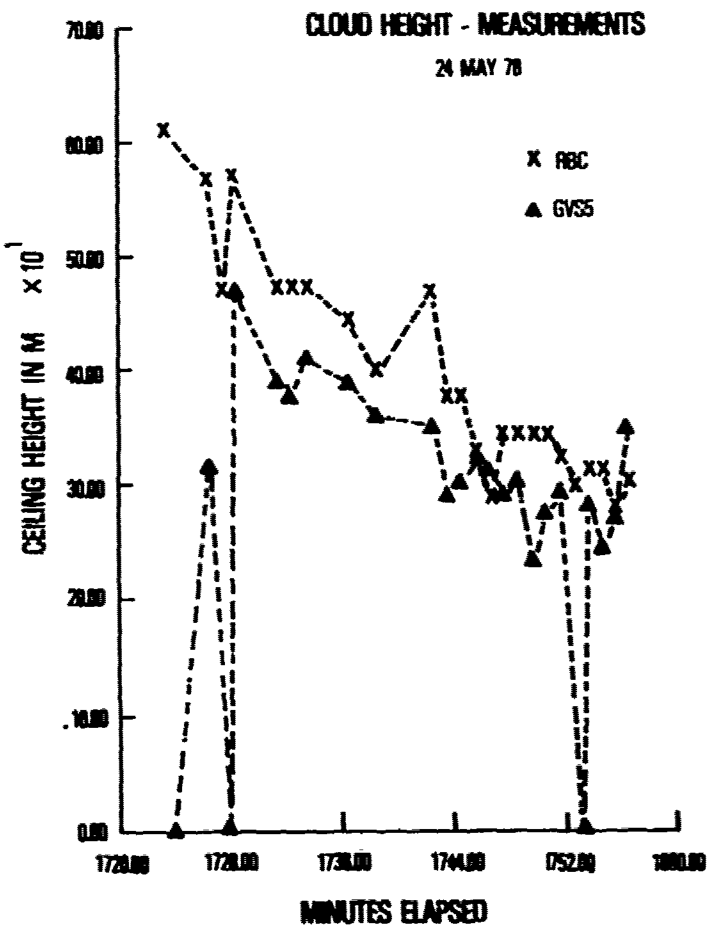

Figure 12. Comparison of the AN/GVS-5 to the RBC.

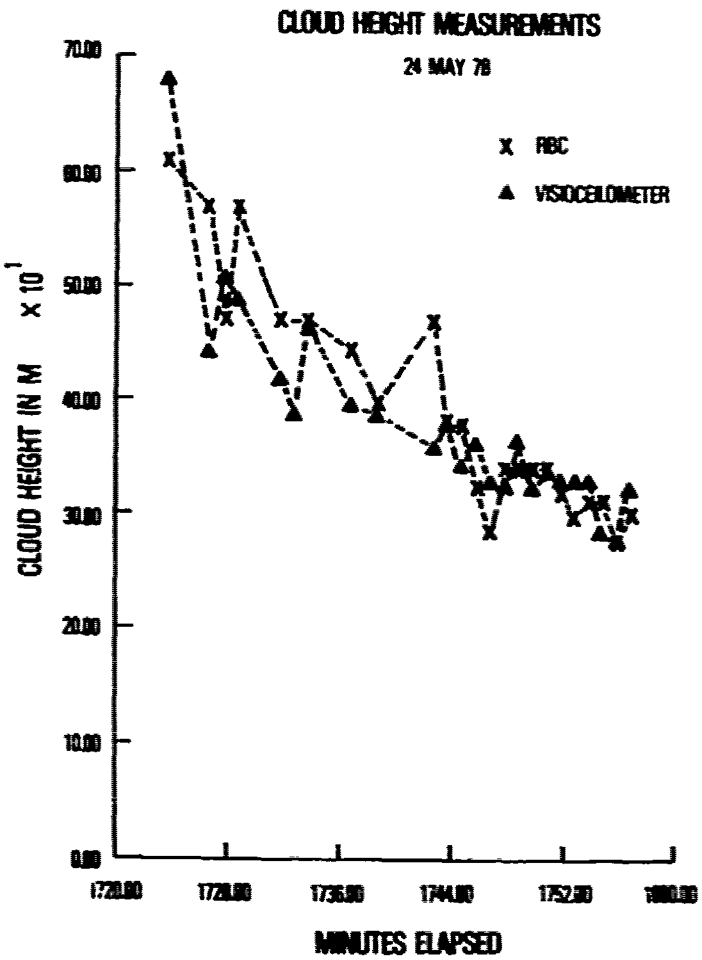

Figure 13. Comparison of the visioceilometer to the RBC.

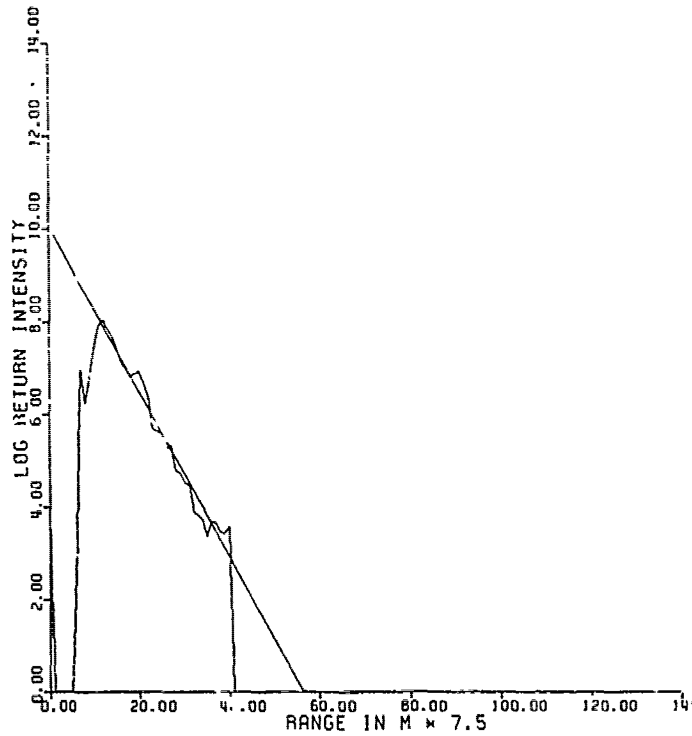

Figure 14. Linear least squares fit to backscatter return.

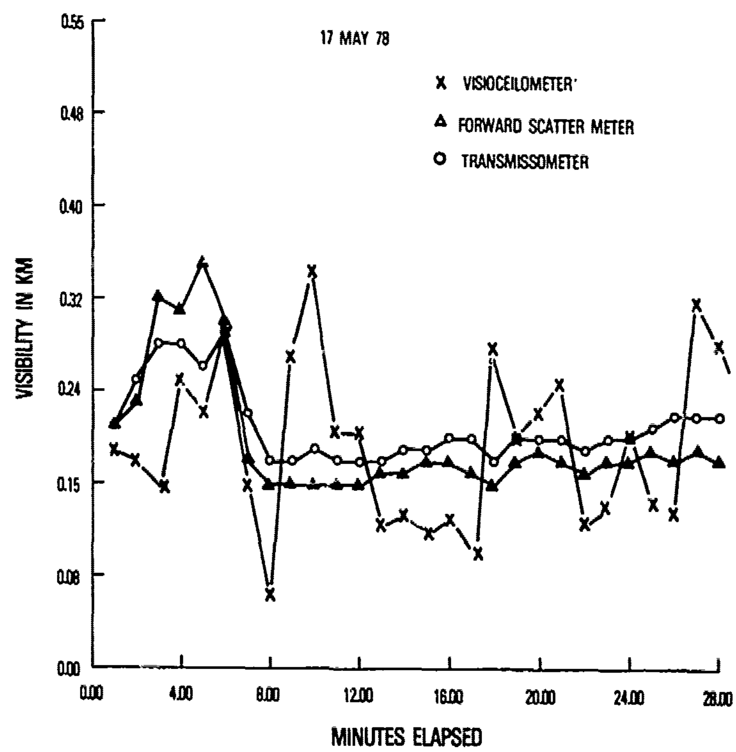

Figure 15. Visibility measurement comparisons of the visioceilometer, forward scatter meter, and transmissometer.

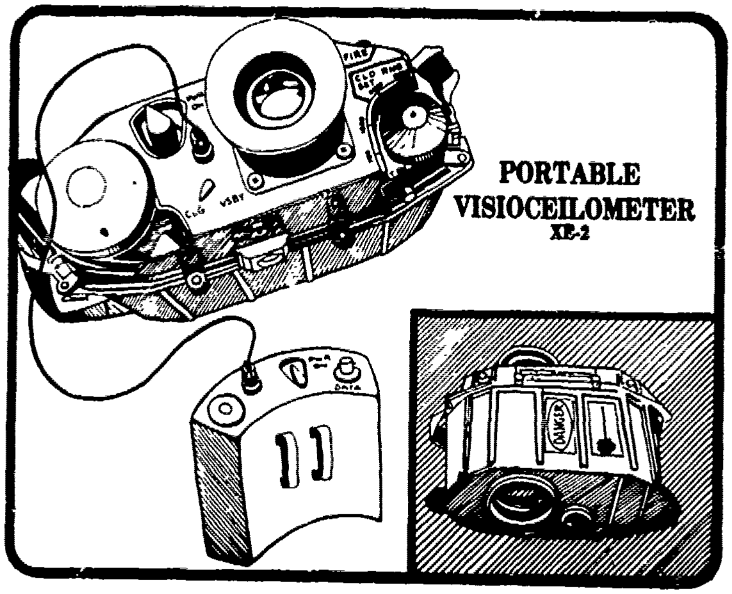

Figure 16. Portable visioceilometer (model-2).

REFERENCES

1. Bonner, R. S., and R. Newton, 1977, "Application of the AN/GVS-5 Laser Rangefinder to Cloud Base Height Measurements," ECOM-5812, Atmospheric Sciences Laboratory, White Sands Missile Range, NM.

2. Saphow, Henry, Fred Kolylarz, Gunther Kaindz, and Earl Griggs, 1979, "The Visioceilometer (XE1) ANGMQ ( ) (Visibility and Ceiling Sensor)," draft report, US Army Electronics Command, Fort Monmouth, NJ.

3. Middleton, W. E. K., 1963, Vision Through the Atmosphere, Toronto Press, Toronto, Canada.

4. Viezee, William, et al, 1972, "Slant Range Visibility Measurement for Aircraft Landing Operations," AFCRL-72-DI54.

5. Viezee, W., E. Uthe, and R. T. H. Collis, 1969, "Lidar Observations of Airfield Approach Conditions: An Exploratory Study," JAM, 2:274-283.

6. Viezee, William, L. Oblanas, and R. T. H. Collis, 1973, "Evaluation of the Lidar Technique of Determining Slant Range Visibility for Aircraft Landing Operations," AFCRL-TR-73-0708, Air Force Cambridge Research Laboratories, Bedford, MA.

7. Blattner, W. G. M., and C. M. Lampley, 1977, "Multiple Scattering Effects for Backscatter Lidar System at WSMR," Radiation Research Associates, RRA-47706, Fort Worth, TX.

8. Douglas, C. A., and R. L. Booker, 1977, "Visual Range: Concepts, Instrumental Determination, and Aviation Applications," FAA-RD-77-8 AD A 041098.

9. Hering, Wayne S., and E. B. Geilser, 1978, "Forward Scatter Meter Measurements of Slant Visual Range," AFGL-TR-78-0191, Air Force Geophysical Laboratory, Hanscom AFB, MA.

10. Hering, Wayne S., H. S. Muench, and H. A. Brown, 1971, "Field Test of a Forward Scatter Visibility Meter," AFCRL-71-0315, AD726995, Air Force Cambridge Research Laboratories, Bedford, MA.

11. Trusty, G. L., and T. H. Cosden, 1979, "Optical Extinction Predictions from Measurements on the Open Sea," NRL Report 8260, Naval Research Laboratory, Washington, DC.

12. Bonner, R. S., SFC R. W. Carroll, and SP5 D. R. McWilliams, 1976, "Ceilometer, Type QL-1210, Ceiloskip, and Videograph B," Foreign Materiel Exploitation Report AST-1740A-096-76, White Sands Missile Range, NM.

DISTRIBUTION LIST

Dr. Frank D. Eaton
Geophysical Institute
University of Alaska
Fairbanks, AK 99701

Commander
US Army Aviation Center
ATTN: ATZQ-D-MA
Fort Rucker, AL 36362

Chief, Atmospheric Sciences Div
Code ES-81
NASA
Marshall Space Flight Center,
AL 35812

Commander
US Army Missile R&D Command
ATTN: DRDMI-CGA (B. W. Fowler)
Redstone Arsenal, AL 35809

Redstone Scientific Information Center
ATTN: DRDMI-TBD
US Army Missile R&D Command
Redstone Arsenal, AL 35809

Commander
US Army Missile R&D Command
ATTN: DRDMI-TEM (R. Haraway)
Redstone Arsenal, AL 35809

Commander
US Army Missile R&D Command
ATTN: DRDMI-TRA (Dr. Essenwanger)
Redstone Arsenal, AL 35809

Commander
HQ, Fort Huachuca
ATTN: Tech Ref Div
Fort Huachuca, AZ 85613

Commander
US Army Intelligence Center & School
ATTN: ATSI-CD-MD
Fort Huachuca, AZ 85613

Commander
US Army Yuma Proving Ground
ATTN: Technical Library
Bldg 2100
Yuma, AZ 85364

Naval Weapons Center (Code 3173)
ATTN: Dr. A. Shlanta
China Lake, CA 93555

Sylvania Elec Sys Western Div
ATTN: Technical Reports Library
PO Box 205
Mountain View, CA 94040

Geophysics Officer
PMTC Code 3250
Pacific Missile Test Center
Point Mugu, CA 93042

Commander
Naval Ocean Systems Center (Code 4473)
ATTN: Technical Library
San Diego, CA 92152

Meteorologist in Charge
Kwajalein Missile Range
PO Box 67
APO San Francisco, CA 96555

Director
NOAA/ERL/APCL R31
RB3-Room 567
Boulder, CO 80302

Library-R-51-Tech Reports
NOAA/ERL
320 S. Broadway
Boulder, CO 80302

National Center for Atmos Research
NCAR Library
PO Box 3000
Boulder, CO 80307

R. B. Girardo
Bureau of Reclamation
E&R Center, Code 1220
Denver Federal Center, Bldg 67
Denver, CO 80225

National Weather Service
National Meteorological Center
W321, WWB, Room 201
ATTN: Mr. Quiroz
Washington, DC 20233

Mil Assistant for Atmos Sciences
Ofc of the Undersecretary of Defense
for Rsch & Engr/E&LS - Room 3D129
The Pentagon
Washington, DC 20301

Defense Communications Agency
Technical Library Center
Code 205
Washington, DC 20305

Director
Defense Nuclear Agency
ATTN: Technical Library
Washington, DC 20305

HQDA (DAEN-RDM/Dr. de Percin)
Washington, DC 20314

Director
Naval Research Laboratory
Code 5530
Washington, DC 20375

Commanding Officer
Naval Research Laboratory
Code 2627
Washington, DC 20375

Dr. J. M. MacCallum
Naval Research Laboratory
Code 1409
Washington, DC 20375

The Library of Congress
ATTN: Exchange & Gift Div
Washington, DC 20540
2

Head, Atmos Rsch Section
Div Atmospheric Science
National Science Foundation
1800 G. Street, NW
Washington, DC 20550

CPT Hugh Albers, Exec Sec
Interdept Committee on Atmos Science
National Science Foundation
Washington, DC 20550

Director, Systems R&D Service
Federal Aviation Administration
ATTN: ARD-54
2100 Second Street, SW
Washington, DC 20590

ADTC/DLODL
Eglin AFB, FL 32542

Naval Training Equipment Center
ATTN: Technical Library
Orlando, FL 32813

Det 11, 2WS/OI
ATTN: Maj Orondorff
Patrick AFB, FL 32925

USAFETAC/CB
Scott AFB, IL 62225

HQ, ESD/TOSI/S-22
Hanscom AFB, MA 01731

Air Force Geophysics Laboratory
ATTN: LCB (A. S. Carten, Jr.)
Hanscom AFB, MA 01731

Air Force Geophysics Laboratory
ATTN: LYD
Hanscom AFB, MA 01731

Meteorology Division
AFGL/LY
Hanscom AFB, MA 01731

US Army Liaison Office
MIT-Lincoln Lab, Library A-082
PO Box 73
Lexington, MA 02173

Director
US Army Ballistic Rsch Lab
ATTN: DRDAR-BLB (Dr. G. E. Keller)
Aberdeen Proving Ground, MD 21005

Commander
US Army Ballistic Rsch Lab
ATTN: DRDAR-BLP
Aberdeen Proving Ground, MD 21005

Director
US Army Armament R&D Command
Chemical Systems Laboratory
ATTN: DRDAR-CLJ-I
Aberdeen Proving Ground, MD 21010

Chief CB Detection & Alarms Div
Chemical Systems Laboratory
ATTN: DRDAR-CLC-CR (H. Tannenbaum)
Aberdeen Proving Ground, MD 21010

Commander
Harry Diamond Laboratories
ATTN: DELHD-CO
2800 Powder Mill Road
Adelphi, MD 20783

Commander
ERADCOM
ATTN: DRDEL-AP
2800 Powder Mill Road
Adelphi, MD 20783
2

Commander
ERADCOM
ATTN: DRDEL-CG/DRDEL-DC/DRDEL-CS
2800 Powder Mill Road
Adelphi, MD 20783

Commander
ERADCOM
ATTN: DRDEL-CT
2800 Powder Mill Road
Adelphi, MD 20783

Commander
ERADCOM
ATTN: DRDEL-EA
2800 Powder Mill Road
Adelphi, MD 20783

Commander
ERADCOM
ATTN: DRDEL-PA/DRDEL-ILS/DRDEL-E
2800 Powder Mill Road
Adelphi, MD 20783

Commander
ERADCOM
ATTN: DRDEL-PAO (S. Kimmel)
2800 Powder Mill Road
Adelphi, MD 20783

Chief
Intelligence Materiel Dev & Support Ofc
ATTN: DELEW-WL-I
Bldg 4554
Fort George G. Meade, MD 20755

Acquisitions Section, IRDB-D823
Library & Info Service Div, NOAA
6009 Executive Blvd
Rockville, MD 20852

Naval Surface Weapons Center
White Oak Library
Silver Spring, MD 20910

The Environmental Research
Institute of MI
ATTN: IRIA Library
PO Box 8618
Ann Arbor, MI 48107

Mr. William A. Main
USDA Forest Service
1407 S. Harrison Road
East Lansing, MI 48823

Dr. A. D. Belmont
Research Division
PO Box 1249
Control Data Corp
Minneapolis, MN 55440

Director
Naval Oceanography & Meteorology
NSTL Station
Bay St Louis, MS 39529

Director
US Army Engr Waterways Experiment Sta
ATTN: Library
PO Box 631
Vicksburg, MS 39180

Environmental Protection Agency
Meteorology Laboratory
Research Triangle Park, NC 27711

US Army Research Office
ATTN: DRXRO-PP
PO Box 12211
Research Triangle Park, NC 27709

Commanding Officer
US Army Armament R&D Command
ATTN: DRDAR-TSS Bldg 59
Dover, NJ 07801

Commander
HQ, US Army Avionics R&D Activity
ATTN: DAVAA-O
Fort Monmouth, NJ 07703

Commander/Director
US Army Combat Surveillance & Target Acquisition Laboratory
ATTN: DELCS-D
Fort Monmouth, NJ 07703

Commander
US Army Electronics R&D Command
ATTN: DELCS-S
Fort Monmouth, NJ 07703

US Army Materiel Systems Analysis Activity
ATTN: DRXSY-MP
Aberdeen Proving Ground, MD 21005

Director
US Army Electronics Technology & Devices Laboratory
ATTN: DELET-D
Fort Monmouth, NJ 07703

Commander
US Army Electronic Warfare Laboratory
ATTN: DELEW-D
Fort Monmouth, NJ 07703

Commander
US Army Night Vision & Electro-Optics Laboratory
ATTN: DELNV-L (Dr. Rudolf Buser)
Fort Monmouth, NJ 07703

Commander
ERADCOM Technical Support Activity
ATTN: DELSD-L
Fort Monmouth, NJ 07703

Project Manager, FIREFINDER
ATTN: DRCPM-FF
Fort Monmouth, NJ 07703

Project Manager, REMBASS
ATTN: DRCPM-RBS
Fort Monmouth, NJ 07703

Commander
US Army Satellite Comm Agency
ATTN: DRCPM-SC-3
Fort Monmouth, NJ 07703

Commander
ERADCOM Scientific Advisor
ATTN: DRDEL-SA
Fort Monmouth, NJ 07703

6585 TG/WE
Holloman AFB, NM 88330

AFWL/WE
Kirtland, AFB, NM 87117

AFWL/Technical Library (SUL)
Kirtland AFB, NM 87117

Commander
US Army Test & Evaluation Command
ATTN: STEWS-AD-L
White Sands Missile Range, NM 88002

Rome Air Development Center
ATTN: Documents Library
TSLD (Bette Smith)
Griffiss AFB, NY 13441

Commander
US Army Tropic Test Center
ATTN: STETC-TD (Info Center)
APO New York 09827

Commandant
US Army Field Artillery School
ATTN: ATSF-CD-R (Mr. Farmer)
Fort Sill, OK 73503

Commandant
US Army Field Artillery School
ATTN: ATSF-CF-R
Fort Sill, OK 73503

Director CFD
US Army Field Artillery School
ATTN: Met Division
Fort Sill, OK 73503

Commandant
US Army Field Artillery School
ATTN: Morris Swett Library
Fort Sill, OK 73503

Commander
US Army Dugway Proving Ground
ATTN: MT-DA-L
Dugway, UT 84022

Dr. C. R. Sreedrahan
Research Associates
Utah State University, UNC 48
Logan, UT 84322

Inge Dirmhirn, Professor
Utah State University, UNC 48
Logan, UT 84322

Defense Documentation Center
ATTN: DDC-TCA
Cameron Station Bldg 5
Alexandria, VA 22314
12

Commanding Officer
US Army Foreign Sci & Tech Center
ATTN: DRXST-IS1
220 7th Street, NE
Charlottesville, VA 22901

Naval Surface Weapons Center
Code G65
Dahlgren, VA 22448

Commander
US Army Night Vision
& Electro-Optics Lab
ATTN: DELNV-D
Fort Belvoir, VA 22060

Commander and Director
US Army Engineer Topographic Lab
ETL-TD-MB
Fort Belvoir, VA 22060

Director
Applied Technology Lab
DAVDL-EU-TSD
ATTN: Technical Library
Fort Eustis, VA 23604

Department of the Air Force
OL-C, 5WW
Fort Monroe, VA 23651

Department of the Air Force
5WW/DN
Langley AFB, VA 23665

Director
Development Center MCDEC
ATTN: Firepower Division
Quantico, VA 22134

US Army Nuclear & Chemical Agency
ATTN: MONA-WE
Springfield, VA 22150

Director
US Army Signals Warfare Laboratory
ATTN: DELSW-OS (Dr. R. Burkhardt)
Vint Hill Farms Station
Warrenton, VA 22186

Commander
US Army Cold Regions Test Center
ATTN: STECR-OP-PM
APO Seattle, WA 98733

Dr. John L. Walsh
Code 5560
Navy Research Lab
Washington, DC 20375

Commander
TRASANA
ATTN: ATAA-PL
(Dolores Anguiano)
White Sands Missile Range, NM 88002

Commander
US Army Dugway Proving Ground
ATTN: STEDP-MT-DA-M (Mr. Paul Carlson)
Dugway, UT 84022

Commander
US Army Dugway Proving Ground
ATTN: STEDP-MT-DA-T
(Mr. William Peterson)
Dugway, UT 84022

Commander
USATRADOC
ATTN: ATCD-SIE
Fort Monroe, VA 23651

Commander
USATRADOC
ATTN: ATCD-CF
Fort Monroe, VA 23651

Commander
USATRADOC
ATTN: Tech Library
Fort Monroe, VA 23651

ATMOSPHERIC SCIENCES RESEARCH PAPERS

1. Lindberg, J.D., "An Improvement to a Method for Measuring the Absorption Coefficient of Atmospheric Dust and other Strongly Absorbing Powders, " ECOM-5565, July 1975.
2. Avara, Elton, P., "Mesoscale Wind Shears Derived from Thermal Winds," ECOM-5566, July 1975.
3. Gomez, Richard B., and Joseph H. Pierluissi, "Incomplete Gamma Function Approximation for King's Strong-Line Transmittance Model," ECOM-5567, July 1975.
4. Blanco, A.J., and B.F. Engebos, "Ballistic Wind Weighting Functions for Tank Projectiles," ECOM-5568, August 1975.
5. Taylor, Fredrick J., Jack Smith, and Thomas H. Pries, "Crosswind Measurements through Pattern Recognition Techniques," ECOM-5569, July 1975.
6. Walters, D.L., "Crosswind Weighting Functions for Direct-Fire Projectiles," ECOM-5570, August 1975.
7. Duncan, Louis D., "An Improved Algorithm for the Iterated Minimal Information Solution for Remote Sounding of Temperature," ECOM-5571, August 1975.
8. Robbiani, Raymond L., "Tactical Field Demonstration of Mobile Weather Radar Set AN/TPS-41 at Fort Rucker, Alabama," ECOM-5572, August 1975.
9. Miers, B., G. Blackman, D. Langer, and N. Lorimier, "Analysis of SMS/GOES Film Data," ECOM-5573, September 1975.
10. Manquero, Carlos, Louis Duncan, and Rufus Bruce, "An Indication from Satellite Measurements of Atmospheric CO2 Variability," ECOM-5574, September 1975.
11. Petracca, Carmine, and James D. Lindberg, "Installation and Operation of an Atmospheric Particulate Collector," ECOM-5575, September 1975.
12. Avara, Elton P., and George Alexander, "Empirical Investigation of Three Iterative Methods for Inverting the Radiative Transfer Equation," ECOM-5576, October 1975.
13. Alexander, George D., "A Digital Data Acquisition Interface for the SMS Direct Readout Ground Station — Concept and Preliminary Design," ECOM-5577, October 1975.
14. Cantor, Israel, "Enhancement of Point Source Thermal Radiation Under Clouds in a Nonattenuating Medium," ECOM-5578, October 1975.
15. Norton, Colburn, and Glenn Hoidale, "The Diurnal Variation of Mixing Height by Month over White Sands Missile Range, N.M," ECOM-5579, November 1975.
16. Avara, Elton P., "On the Spectrum Analysis of Binary Data," ECOM-5580, November 1975.
17. Taylor, Fredrick J., Thomas H. Pries, and Chao-Huan Huang, "Optimal Wind Velocity Estimation," ECOM-5581, December 1975.
18. Avara, Elton P., "Some Effects of Autocorrelated and Cross-Correlated Noise on the Analysis of Variance, " ECOM-5582, December 1975.
19. Gillespie, Patti S., R.L. Armstrong, and Kenneth O. White, "The Spectral Characteristics and Atmospheric CO2 Absorption of the Ho^{+3}:YLF Laser at 2.05μm," ECOM-5583, December 1975.
20. Novlan, David J. "An Empirical Method of Forecasting Thunderstorms for the White Sands Missile Range," ECOM-5584, February 1976.
21. Avara, Elton P., "Randomization Effects in Hypothesis Testing with Autocorrelated Noise," ECOM-5585, February 1976.
22. Watkins, Wendell R., "Improvements in Long Path Absorption Cell Measurement," ECOM-5586, March 1976.
23. Thomas, Joe, George D. Alexander, and Marvin Dubbin, "SATTEL — An Army Dedicated Meteorological Telemetry System," ECOM-5587. March 1976.
24. Kennedy, Bruce W., and Delbert Bynum, "Army User Test Program for the RDT&E-XM-75 Meteorological Rocket," ECOM-5588, April 1976.

25. Barnett, Kenneth M., "A Description of the Artillery Meteorological Comparisons at White Sands Missle Range, October 1974 - December 1974 ('PASS' - Prototype Artillery [Meteorological] Subsystem)," ECOM-5589, April 1976.
26. Miller, Walter B., "Preliminary Analysis of Fall-of-Shot From Project 'PASS'," ECOM-5590, April 1976.
27. Avara, Elton P., "Error Analysis of Minimum Information and Smith's Direct Methods for Inverting the Radiative Transfer Equation," ECOM-5591, April 1976.
28. Yee, Young P., James D. Horn, and George Alexander, "Synoptic Thermal Wind Calculations from Radiosonde Observations Over the Southwestern United States," ECOM-5592, May 1976.
29. Duncan, Louis D., and Mary Ann Seagraves, "Applications of Empirical Corrections to NOAA-4 VTPR Observations," ECOM-5593, May 1976.
30. Miers, Bruce T., and Steve Weaver, "Applications of Meterological Satellite Data to Weather Sensitive Army Operations,"ECOM-5594, May 1976.
31. Sharenow, Moses, "Redesign and Improvement of Balloon ML-566," ECOM-5595, June, 1976.
32. Hansen, Frank V., "The Depth of the Surface Boundary Layer," ECOM-5596, June 1976.
33. Pinnick, R.G., and E.B. Stenmark, "Response Calculations for a Commercial Light-Scattering Aerosol Counter," ECOM-5597, July 1976.
34. Mason, J., and G.B. Hoidale, "Visibility as an Estimator of Infrared Transmittance," ECOM-5598, July 1976.
35. Bruce, Rufus E., Louis D. Duncan, and Joseph H. Pierluissi, "Experimental Study of the Relationship Between Radiosonde Temperatures and Radiometric-Area Temperatures," ECOM-5599, August 1976.
36. Duncan, Louis D., "Stratospheric Wind Shear Computed from Satellite Thermal Sounder Measurements," ECOM-5800, September 1976.
37. Taylor, F., P. Mohan, P. Joseph and T. Pries, "An All Digital Automated Wind Measurement System," ECOM-5801, September 1976.
38. Bruce, Charles, "Development of Spectrophones for CW and Pulsed Radiation Sources," ECOM-5802, September 1976.
39. Duncan, Louis D., and Mary Ann Seagraves,"Another Method for Estimating Clear Column Radiances," ECOM-5803, October 1976.
40. Blanco, Abel J., and Larry E. Taylor, "Artillery Meteorological Analysis of Project Pass," ECOM-5804, October 1976.
41. Miller, Walter, and Bernard Engebos," A Mathematical Structure for Refinement of Sound Ranging Estimates," ECOM-5805, November, 1976.
42. Gillespie, James B., and James D. Lindberg, "A Method to Obtain Diffuse Reflectance Measurements from 1.0 to 3.0 μm Using a Cary 17I Spectrophotometer," ECOM-5806, November 1976.
43. Rubio, Roberto, and Robert O. Olsen,"A Study of the Effects of Temperature Variations on Radio Wave Absorption,"ECOM-5807, November 1976.
44. Ballard, Harold N., "Temperature Measurements in the Stratosphere from Balloon-Borne Instrument Platforms, 1968-1975," ECOM-5808, December 1976.
45. Monahan, H.H., "An Approach to the Short-Range Prediction of Early Morning Radiation Fog," ECOM-5809, January 1977.
46. Engebos, Bernard Francis, "Introduction to Multiple State Multiple Action Decision Theory and Its Relation to Mixing Structures," ECOM-5810, January 1977.
47. Low, Richard D.H.,"Effects of Cloud Particles on Remote Sensing from Space in the 10-Micrometer Infrared Region," ECOM-5811, January 1977.
48. Bonner, Robert S., and R. Newton, "Application of the AN/GVS-5 Laser Rangefinder to Cloud Base Height Measurements," ECOM-5812, February 1977.
49. Rubio, Roberto, "Lidar Detection of Subvisible Reentry Vehicle Erosive Atmospheric Material," ECOM-5813, March 1977.
50. Low, Richard D.H., and J.D. Horn, "Mesoscale Determination of Cloud-Top Height: Problems and Solutions," ECOM-5814, March 1977.

51. Duncan, Louis D., and Mary Ann Seagraves,"Evaluation of the NOAA-4 VTPR Thermal Winds for Nuclear Fallout Predictions," ECOM-5815, March 1977.
52. Randhawa, Jagir S., M. Izquierdo, Carlos McDonald and Zvi Salpeter, "Stratospheric Ozone Density as Measured by a Chemiluminescent Sensor During the Stratcom VI-A Flight," ECOM-5816, April 1977.
53. Rubio, Roberto, and Mike Izquierdo, "Measurements of Net Atmospheric Irradiance in the 0.7- to 2.8-Micrometer Infrared Region," ECOM-5817, May 1977.
54. Ballard, Harold N., Jose M. Serna, and Frank P. Hudson Consultant for Chemical Kinetics, "Calculation of Selected Atmospheric Composition Parameters for the Mid-Latitude, September Stratosphere," ECOM-5818, May 1977.
55. Mitchell, J.D., R.S. Sagar, and R.O. Olsen, "Positive Ions in the Middle Atmosphere During Sunrise Conditions," ECOM-5819, May 1977.
56. White, Kenneth O., Wendell R. Watkins, Stuart A. Schleusener, and Ronald L. Johnson, "Solid-State Laser Wavelength Identification Using a Reference Absorber," ECOM-5820, June 1977.
57. Watkins, Wendell R., and Richard G. Dixon, "Automation of Long-Path Absorption Cell Measurements," ECOM-5821, June 1977.
58. Taylor, S.E., J.M. Davis, and J.B. Mason, "Analysis of Observed Soil Skin Moisture Effects on Reflectance," ECOM-5822, June 1977.
59. Duncan, Louis D. and Mary Ann Seagraves, "Fallout Predictions Computed from Satellite Derived Winds," ECOM-5823, June 1977.
60. Snider, D.E., D.G. Murcray, F.H. Murcray, and W.J. Williams, "Investigation of High-Altitude Enhanced Infrared Backround Emissions" (U), SECRET, ECOM-5824, June 1977.
61. Dubbin, Marvin H., and Dennis Hall, "Synchronous Meteorlogical Satellite Direct Readout Ground System Digital Video Electronics," ECOM-5825, June 1977.
62. Miller, W., and B. Engebos, "A Preliminary Analysis of Two Sound Ranging Algorithms," ECOM-5826, July 1977.
63. Kennedy, Bruce W., and James K. Luers, "Ballistic Sphere Techniques for Measuring Atomspheric Parameters," ECOM-5827, July 1977.
64. Duncan, Louis D., "Zenith Angle Variation of Satellite Thermal Sounder Measurements," ECOM-5828, August 1977.
65. Hansen, Frank V., "The Critical Richardson Number," ECOM-5829, September 1977.
66. Ballard, Harold N., and Frank P. Hudson (Compilers), "Stratospheric Composition Balloon-Borne Experiment," ECOM-5830, October 1977.
67. Barr, William C., and Arnold C. Peterson, "Wind Measuring Accuracy Test of Meteorological Systems," ECOM-5831, November 1977.
68. Ethridge, G.A. and F.V. Hansen, "Atmospheric Diffusion: Similarity Theory and Empirical Derivations for Use in Boundary Layer Diffusion Problems," ECOM-5832, November 1977.
69. Low, Richard D.H., "The Internal Cloud Radiation Field and a Technique for Determining Cloud Blackness," ECOM-5833, December 1977.
70. Watkins, Wendell R., Kenneth O. White, Charles W. Bruce, Donald L. Walters, and James D. Lindberg, "Measurements Required for Prediction of High Energy Laser Transmission," ECOM-5834, December 1977.
71. Rubio, Robert, "Investigation of Abrupt Decreases in Atmospherically Backscattered Laser Energy," ECOM-5835, December 1977.
72. Monahan, H.H. and R.M. Cionco, "An Interpretative Review of Existing Capabilities for Measuring and Forecasting Selected Weather Variables (Emphasizing Remote Means)," ASL-TR-0001, January 1978.
73. Heaps, Melvin G., "The 1979 Solar Eclipse and Validation of D-Region Models," ASL-TR-0002, March 1978.

74. Jennings, S.G., and J.B. Gillespie, "M.I.E. Theory Sensitivity Studies - The Effects of Aerosol Complex Refractive Index and Size Distribution Variations on Extinction and Absorption Coefficients Part II: Analysis of the Computational Results," ASL-TR-0003, March 1978.

75. White, Kenneth O. et al, "Water Vapor Continuum Absorption in the 3.5μm to 4.0μm Region," ASL-TR-0004, March 1978.

76. Olsen, Robert O., and Bruce W. Kennedy, "ABRES Pretest Atmospheric Measurements," ASL-TR-0005, April 1978.

77. Ballard, Harold N., Jose M. Serna, and Frank P. Hudson, "Calculation of Atmospheric Composition in the High Latitude September Stratosphere," ASL-TR-0006, May 1978.

78. Watkins, Wendell R. et al, "Water Vapor Absorption Coefficients at HF Laser Wavelengths," ASL-TR-0007, May 1978.

79. Hansen, Frank V., "The Growth and Prediction of Nocturnal Inversions," ASL-TR-0008, May 1978.

80. Samuel, Christine, Charles Bruce, and Ralph Brewer, "Spectrophone Analysis of Gas Samples Obtained at Field Site," ASL-TR-0009, June 1978.

81. Pinnick, R.G. et al., "Vertical Structure in Atmospheric Fog and Haze and its Effects on IR Extinction," ASL-TR-0010, July 1978.

82. Low, Richard D.H., Louis D. Duncan, and Richard B. Gomez, "The Microphysical Basis of Fog Optical Characterization," ASL-TR-0011, August 1978.

83. Heaps, Melvin G., "The Effect of a Solar Proton Event on the Minor Neutral Constituents of the Summer Polar Mesosphere," ASL-TR-0012, August 1978.

84. Mason, James B., "Light Attenuation in Falling Snow," ASL-TR-0013, August 1978.

85. Blanco, Abel J., "Long-Range Artillery Sound Ranging: "PASS" Meteorological Application," ASL-TR-0014, September 1978.

86. Heaps, M.G., and F.E. Niles, "Modeling the Ion Chemistry of the D-Region: A case Study Based Upon the 1966 Total Solar Eclipse," ASL-TR-0015, September 1978.

87. Jennings, S.G., and R.G. Pinnick, "Effects of Particulate Complex Refractive Index and Particle Size Distribution Variations on Atmospheric Extinction and Absorption for Visible Through Middle-Infrared Wavelengths," ASL-TR-0016, September 1978.

88. Watkins, Wendell R., Kenneth O. White, Lanny R. Bower, and Brian Z. Sojka, " Pressure Dependence of the Water Vapor Continuum Absorption in the 3.5- to 4.0-Micrometer Region," ASL-TR-0017, September 1978.

89. Miller, W.B., and B.F. Engebos, "Behavior of Four Sound Ranging Techniques in an Idealized Physical Enviroment," ASL-TR-0018, September 1978.

90. Gomez, Richard G., "Effectiveness Studies of the CBU-88/B Bomb, Cluster, Smoke Weapon" (U), CONFIDENTIAL ASL-TR-0019, September 1978.

91. Miller, August, Richard C. Shirkey, and Mary Ann Seagraves, "Calculation of Thermal Emission from Aerosols Using the Doubling Technique," ASL-TR-0020, November, 1978.

92. Lindberg, James D. et al., "Measured Effects of Battlefield Dust and Smoke on Visible, Infrared, and Millimeter Wavelengths Propagation: A Preliminary Report on Dusty Infrared Test-I (DIRT-I)," ASL-TR-0021, January 1979.

93. Kennedy, Bruce W., Arthur Kinghorn, and B.R. Hixon, "Engineering Flight Tests of Range Meteorological Sounding System Radiosonde," ASL-TR-0022, February 1979.

94. Rubio, Roberto, and Don Hoock, "Microwave Effective Earth Radius Factor Variability at Wiesbaden and Balboa," ASL-TR-0023, February 1979.

95. Low, Richard D.H., "A Theoretical Investigation of Cloud/Fog Optical Properties and Their Spectral Correlations," ASL-TR-0024, February 1979.

96. Pinnick, R.G., and H.J. Auvermann, "Response Characteristics of Knollenberg Light-Scattering Aerosol Counters," ASL-TR-0025, February 1979.
97. Heaps, Melvin G., Robert O. Olsen, and Warren W. Berning, "Solar Eclipse 1979, Atmospheric Sciences Laboratory Program Overview," ASL-TR-0026 February 1979.
98. Blanco, Abel J., "Long-Range Artillery Sound Ranging: 'PASS' GR-8 Sound Ranging Data," ASL-TR-0027, March 1979.
99. Kennedy, Bruce W., and Jose M. Serna, "Meteorological Rocket Network System Reliability," ASL-TR-0028, March 1979.
100. Swingle, Donald M., "Effects of Arrival Time Errors in Weighted Range Equation Solutions for Linear Base Sound Ranging," ASL-TR-0029, April 1979.
101. Umstead, Robert K., Ricardo Pena, and Frank V. Hansen, "KWIK: An Algorithm for Calculating Munition Expenditures for Smoke Screening/Obscuration in Tactical Situations," ASL-TR-0030, April 1979.
102. D'Arcy, Edward M., "Accuracy Validation of the Modified Nike Hercules Radar," ASL-TR-0031, May 1979.
103. Rodriguez, Ruben, "Evaluation of the Passive Remote Crosswind Sensor," ASL-TR-0032, May 1979.
104. Barber, T.L., and R. Rodriguez, "Transit Time Lidar Measurement of Near-Surface Winds in the Atmosphere," ASL-TR-0033, May 1979.
105. Low, Richard D.H., Louis D. Duncan, and Y.Y. Roger R. Hsiao, "Microphysical and Optical Properties of California Coastal Fogs at Fort Ord," ASL-TR-0034, June 1979.
106. Rodriguez, Ruben, and William J. Vechione, "Evaluation of the Saturation Resistant Crosswind Sensor," ASL-TR-0035, July 1979
107. Ohmstede, William D., "The Dynamics of Material Layers," ASL-TR-0036, July 1979.
108. Pinnick, R.G., S.G. Jennings, Petr Chýlek, and H.J. Auvermann "Relationships between IR Extinction, Absorption, and Liquid Water Content of Fogs," ASL-TR-0037, August 1979
109. Rodriguez, Ruben, and William J. Vechione, "Performance Evaluation of the Optical Crosswind Profiler," ASL-TR-0038, August 1979
110. Miers, Bruce T., "Precipitation Estimation Using Satellite Data" ASL-TR-0039, September 1979
111. Dickson, David H., and Charles M. Sonnenschein, "Helicopter Remote Wind Sensor System Description," ASL-TR-0040, September 1979
112. Heaps, Melvin G., and Joseph M. Heimerl, "Validation of the Dairchem Code, I: Quiet Midlatitude Conditions," ASL-TR-0041, September 1979
113. Bonner, Robert S., and William J. Lentz, "The Visioceilometer: A Portable Cloud Height and Visibility Indicator," ASL-TR-0042, October 1979

☆ U.S. GOVERNMENT PRINTING OFFICE: 1979 — 677-119/39